Thermal properties and crystal structures of ruthenium-containing photoreactive ionic liquids with short substituents

Sumitani, Ryo
Funasako, Yusuke
Mochida, Tomoyuki

(Citation)
Journal of Molecular Liquids,318:114071

(Issue Date)
2020-11-15

(Resource Type)
journal article

(Version)
Accepted Manuscript

(URL)
https://hdl.handle.net/20.500.14094/90007777

Thermal Properties and Crystal Structures of Ruthenium-Containing Photoreactive Ionic liquids with Short Substituents

Ryo Sumitani,[a] Yusuke Funasako,[a†] Tomoyuki Mochida*[a,b]

[a]*Department of Chemistry, Graduate School of Science, Kobe University, Rokkodai, Nada, Kobe, Hyogo 657-8501, Japan*

[b]*Center for Membrane Technology, Kobe University, Rokkodai, Nada, Kobe, Hyogo 657-8501, Japan*

**Corresponding author*

E-mail address: tmochida@platinum.kobe-u.ac.jp

[†]Present address: *Department of Applied Chemistry, Faculty of Engineering, Sanyo-Onoda City University, 1-1-1, Daigakudori, Sanyo-Onoda, Yamaguchi 756-0884, Japan*

Graphical abstract

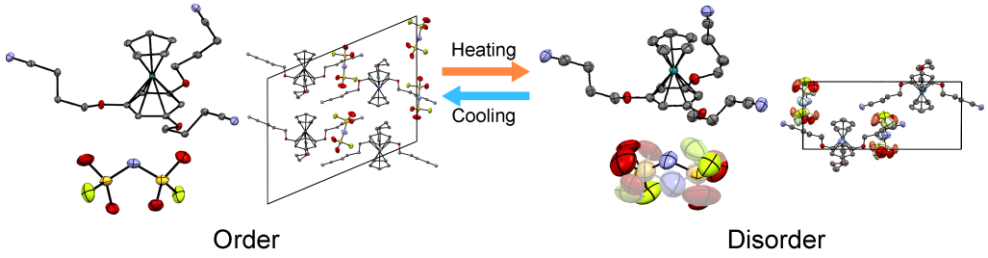

Highlights

· Ionic liquids containing cationic Ru sandwich complexes were synthesized.

· The synthesized salts were solid at ambient temperature and exhibited anion disorder.

· The supercooled liquid of the FSA salt transformed into a coordination polymer upon photoirradiation.

Abstract

To understand the structural features and intermolecular interactions of photoreactive organometallic ionic liquids (ILs), ILs containing cationic Ru sandwich complexes $[Ru(C_5H_5)\{C_6H_3(OC_3H_6CN)_3\}]X$ (**1a**: X = $(FSO_2)_2N^-$, **1b**: X = $(CF_3SO_2)_2N^-$) were synthesized.

Thereafter, their thermal properties and crystal structures were investigated. The melting points of these ILs were determined to be 87 and 79 °C, respectively. In the former crystal, the cation and anion were alternately arranged and the crystal undergoes a phase transition with ordering of the anion at −155 °C. In the latter crystal, the cations formed columnar arrangements through π–π interactions, with the anions located between the columns. In this crystal, the anions were extensively disordered even at −173 °C. The supercooled liquid of **1a** exhibited a photochemical transformation into an amorphous coordination polymer, similar to the IL with longer substituents, though the reaction rate was considerably lower.

Keywords: ionic liquid; crystal structure; ruthenium complex; sandwich complex; order-disorder; phase transition

1. Introduction

Ionic liquids (ILs) are salts whose melting points are below 100 °C. ILs have been extensively studied because of their beneficial applications as solvents and electrolytes [1]. Recently, many ILs containing metal complexes have been synthesized, which exhibit various functions [2]. Further, in our laboratory, we synthesized functional ILs by employing various cationic organometallic and chelate complexes [3,4]. Among them, ILs containing cationic Ru sandwich complexes are transparent, stable, and relatively easy to synthesize [5].

ILs containing Ru sandwich complexes with coordination sites show intriguing photochemical reactivities due to the reactivity of the cation [6,7]. We previously reported that the IL shown in Fig. 1 (IL **1**, T_g = −53 °C) could be converted into an amorphous coordination polymer under ultraviolet (UV) photoirradiation [6]. The cation in this IL possesses three cyanohexyloxy substituents, and the counterion is $(FSO_2)_2N^-$ (FSA). The photoreaction is a novel method of coordination polymer synthesis, and the reaction is reversed upon heating.

Furthermore, the ionic conductivity and viscoelasticity of **1** can be flexibly controlled by photoirradiation and heat treatment [8], thereby paving the way for novel electronic applications. However, the molecular structure and intermolecular interactions of organometallic ILs are not well understood. It is important to find factors that may affect their melting points and viscosities in order to design ILs with higher reactivity.

This study aims to elucidate the structural features of the photoreactive Ru-containing ILs through crystal structure analysis. Elucidation of the structures and conformations of the constituent molecules and the intermolecular interactions in ILs through crystallographic analysis is a versatile approach toward understanding their thermal properties [9]. For example, in the crystals of ILs, the energetically unfavorable conformations and disorders of the molecules result in low melting points. The FSA and $(CF_3SO_2)_2N^-$ (Tf_2N) anions in ILs often display disorder in the solid state [10]. We previously reported that the Ru-containing ILs with 1,2,3-trialkoxybenzene ligands exhibit higher melting points than those with the 1,3,5-substituted ligands owing to the formation of layered structures via the alignment of the alkyl chains [5c]. This result prompted us to choose the 1,3,5-substituted ligand to design the photoreactive ILs. However, there was no structural information for them.

In this paper, we report the thermal properties and crystal structures of ILs **1a** (FSA salt) and **1b** (Tf_2N salt) (Fig. 2). The cation possessed cyanopropyloxy substituents, which were shorter than the cyanohexyloxy substituents in **1**. Therefore, these ILs exhibited higher crystallinity and were suitable for the crystal structure analysis, which provided information about their molecular structures and intermolecular interactions. The supercooled liquid of **1a** exhibited a photochemical transformation into an amorphous coordination polymer, similar to **1**, though the reaction rate was considerably lower. The current investigation confirmed that the cation in **1a** and **1b** did not form a layered structure. It was found that **1a** exhibited a phase transition with ordering of the anion at low temperature, whereas **1b** exhibited extensive anion disorder

even at low temperatures.

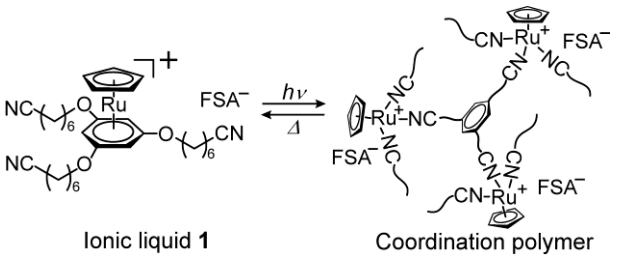

Fig. 1. Reversible transformation between ionic liquid **1** and the amorphous coordination polymer under photoirradiation and heat.

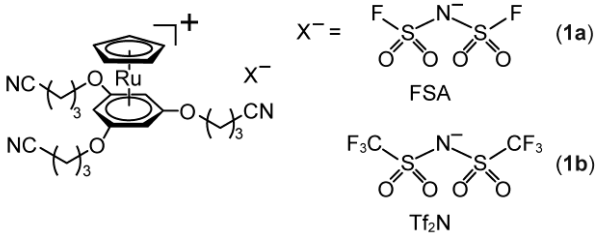

Fig. 2. Structural formulae of **1a** (X = FSA) and **1b** (X = Tf_2N).

2. Results and Discussion

*2.1. Thermal properties of **1a** and **1b***

Differential scanning calorimetry (DSC) measurements of **1a** and **1b** were performed. Both salts were obtained as crystals with melting points of ~80 °C. Upon cooling from the melt, they both underwent a glass transition, at low temperatures.

The DSC trace for **1a** is shown in Fig. 3a. A solid-phase transition (ΔH = 0.3 kJ mol^{-1}, ΔS = 2 J K^{-1} mol^{-1}) was observed at –155.0 °C (Figs. S1), which was found to be an order-disorder transition (see below). This salt melted at 86.9 °C (ΔH_m = 48.1 kJ mol^{-1}, ΔS_m = 133 J K^{-1} mol^{-1}) and did not crystallize upon cooling from the melt, thus showing a glass transition at –26 °C. The DSC trace for **1b** is shown in Fig. 3b. This salt underwent a phase transition in the solid state at 75.0 °C, which was immediately followed by melting at 78.9 °C (ΔH_m = 46.6 kJ mol^{-1}, ΔS_m = 132 J K^{-1} mol^{-1}). Upon cooling from the melt, this salt underwent a glass transition at –

26 °C, and during reheating, partial cold crystallization occurred at 29 °C, which was followed by melting. The ratios of the glass transition temperature to the melting points of **1a** and **1b** are 0.68 and 0.70, respectively, which agree with the empirical relationship (T_g/T_m = 2/3) for molecular compounds [11].

Additionally, the time course of the photoreactivity of **1a** in the liquid state was investigated (Fig. 4). The supercooled liquid of **1a** at 20 °C gradually transformed to an amorphous coordination polymer upon UV photoirradiation, similarly to **1** [6]. However, the reaction rate was considerably lower (~50% conversion in 7 h). This tendency is consistent with the higher glass transition temperature of **1a** (T_g = –26 °C) than that of **1** (T_g = –53 °C [6]), which leads to the higher viscosity of **1a**.

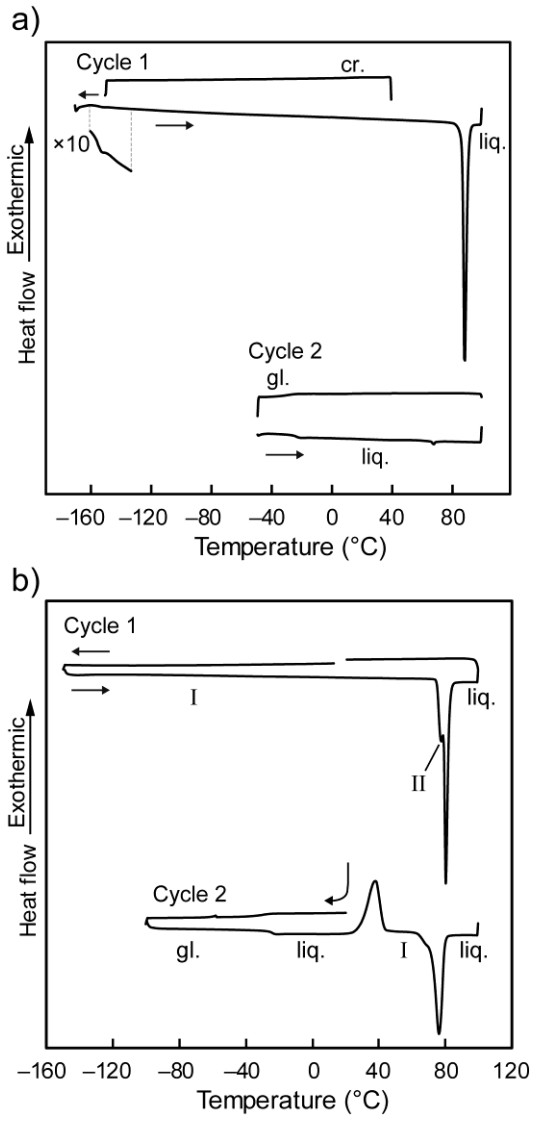

Fig. 3. DSC traces of (a) **1a** and (b) **1b**, where cr., liq., and gl. are the crystal, liquid, and glassy phases, respectively.

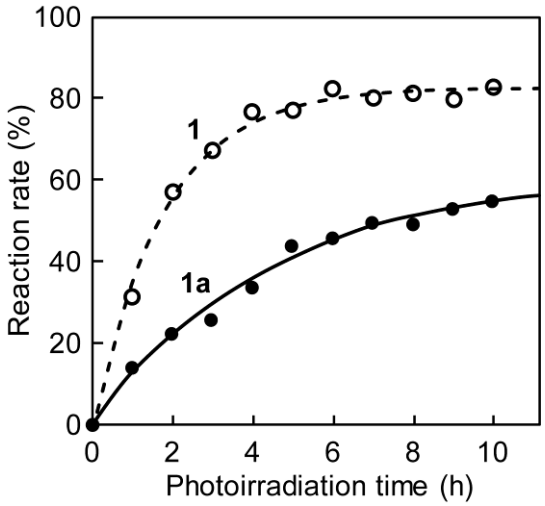

Fig. 4. Time course of the reaction, where the reaction rate is given by the molar ratio of the photoreacted species in the products generated by photoirradiation of **1a** (—) and **1** (--- [6]).

*2.2. Crystal structures of **1a***

The crystal structures of **1a** were determined at −173 and 0 °C, which are below and above the solid phase transition temperature (T_c = −155.0 °C). The analysis revealed that the phase transition accompanied order-disorder of the anion.

The packing diagrams determined at −173 and 0 °C are shown in Figs. 5a and 5b, respectively. The space group was $P2_1/n$ at both temperatures. The cations and anions were arranged alternately in the crystal, and there was no π–π interactions between the cations. There were two pairs of crystallographically independent cations and anions at −173 °C (Z = 8, Fig. 5a), whereas an independent pair existed at 0 °C (Z = 4, Fig. 5b). The *a*-axis was halved in the high-temperature phase as compared to that in the low-temperature phase, accompanied by disordering of the anion. However, the molecular arrangements were almost the same in both

phases.

The molecular structures at these temperatures are shown in Fig. 6. The structures of cation A and anion A are shown in Fig. 6a, while those of cation B and anion B were almost the same (Fig. S2). Moreover, the molecular structures of the cations were almost the same at both temperatures, with larger thermal ellipsoids at 0 °C than at −173 °C. The three substituents in the cation adopted twisted conformations, two of which were outwardly oriented. The coordination structures of the cations were almost identical to those of other Ru sandwich complexes [5]. The anions were ordered at −173 °C and adopted a *transoid* conformation (Fig. 6a). At 0 °C, however, the N atom and the SO_2F moieties exhibited two-fold rotational disorders (occupancy ratios = 0.5:0.5, Fig. 6b). This kind of order-disorder phenomenon of the FSA anion is often observed in the solid state [10].

There were weak intermolecular hydrogen-bond-like interactions between the cyano group of the cation and the arene–H (CH· · · N = 2.46 and 2.55 Å, at −173 °C; 2.56 Å, at 0 °C), as indicated by dotted lines in Fig. 5a, which were 0.2–0.3 Å shorter than the van der Waals (vdW) distance. Similar CN· · · H interactions have been observed in the crystals of imidazolium ILs containing cyanoalkyl substituents [12]. There were hydrogen-bond-like interactions between the cation and anion, Cp–H· · · O, and arene–H· · · O, which were shorter than the vdW distance by > 0.2 Å. Cp stands for the cyclopentadienyl ring. These interactions may raise the melting point of this salt.

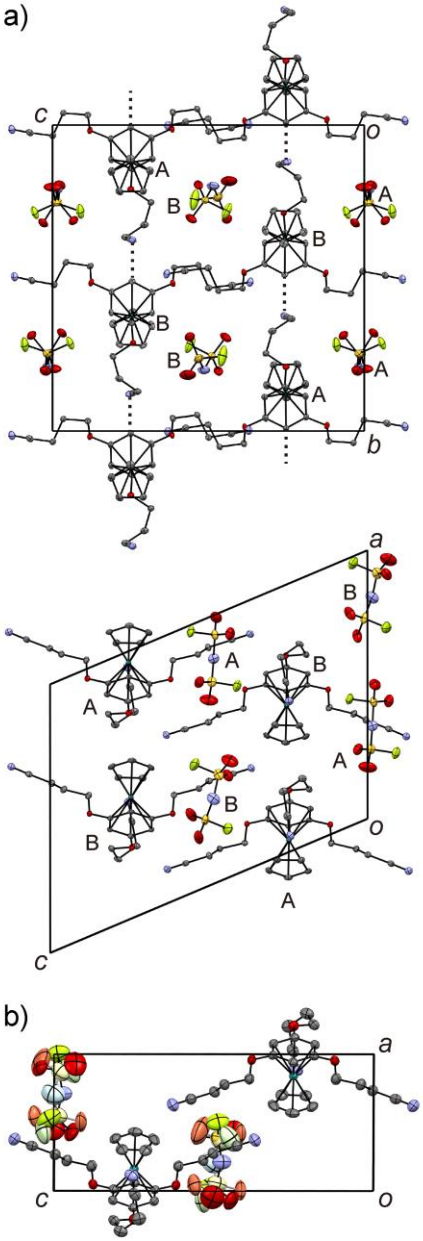

Fig. 5. Packing diagrams of **1a** at (a) −173 and (b) 0 °C. The dotted lines in (a) represent the CN···H interactions.

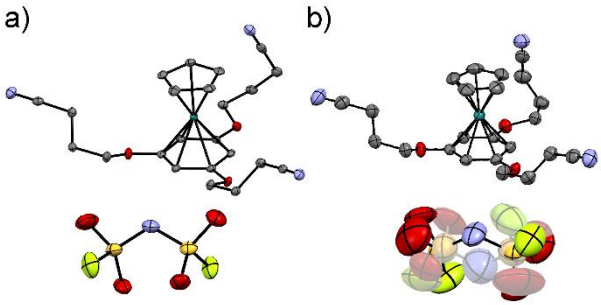

Fig. 6. Molecular structures of **1a** at (a) −173 and (b) 0 °C. The gray part in (b) represents the

disordered moieties with smaller occupancy.

*2.3. Crystal structure of **1b***

The packing diagram of **1b** at –173 °C is shown in Fig. 7a. The space group was $Pca2_1$, and there were two pairs of crystallographically independent cations and anions ($Z = 8$). The cations formed a columnar arrangement through π–π interactions. The anions were not ordered even at this temperature, thus showing severe disorder. The crystal structure was the same at 0 °C.

The structures of cation A and anion A are shown in Fig. 7b. Cation B and anion B possessed almost the same structures as cation A and anion A (Fig. S3), respectively. The substituents in the cation adopted twisted conformations and surrounded the sandwich complex moiety. The cyclopentadienyl (Cp) ring exhibited a rotational two-fold disorder with occupancy ratios of 0.70:0.30 (cation A) and 0.58:0.42 (cation B). The coordination structures of the cations were almost identical to those of other Ru sandwich complexes [5]. The cation in **1b** displayed a more compact substituent arrangement as compared to that in **1a**.

The cations exhibited a columnar arrangement along the *b*-axis, through π–π interactions. The column composed of cation A is shown in Fig. 7c. Cation B also formed a similar column. In the columns, there were two intermolecular C···C contacts between the Cp and arene rings, which were 0.13 Å shorter than the vdW distance (C···C = 3.23, 3.24 Å between cation A and 3.27, 3.26 Å between cation B). The centroid-centroid distances between these rings were 3.77 Å (cation A) and 3.74 Å (cation B). There is a complex with a 1,3,5-substituted arene ligand that shows stronger π–π interactions (Cp–arene centroid-centroid distances: 3.37. 3.43 Å [5c]) than this salt. There were weak hydrogen-bond-like interactions between the columns, as indicated by dotted lines in Fig. 7a. They are between one of the three cyano groups in cation A and the arene–H of cation B in the adjacent column with a distance 0.3 Å shorter than that of vdW (CH···N = 2.48 Å between cations A, and 2.47 Å between cations B). These interactions

may raise the melting point of this salt.

The anion was located between the columns of the cations (Fig. 7a). Between the cation and anion, there were contacts such as $Cp_{(cation\ A)}$–H· · · $O_{(anion\ B)}$ and $arene_{(cation\ B)}$–H· · · $O_{(anion\ A)}$, which were more than 0.2 Å shorter than the vdW distance. The anion adopting the *transoid* conformation exhibited severe disorder, where displacements of the atoms by 0.5 Å (anion A) and 1 Å (anion B) occurred, with occupancy ratios of 0.61:0.39 (anion A) and 0.67:0.33 (anion B). The *transoid* conformation is more stable than the *cisoid* one [13]. Disorder of the Tf_2N anion, which is ordered at low temperatures, is often observed in the solid state [10]. The severe disorder of the current salt even at −173 °C is probably due to the large space in which the anions are located. The extensive anion disorder may lower the melting point of this salt.

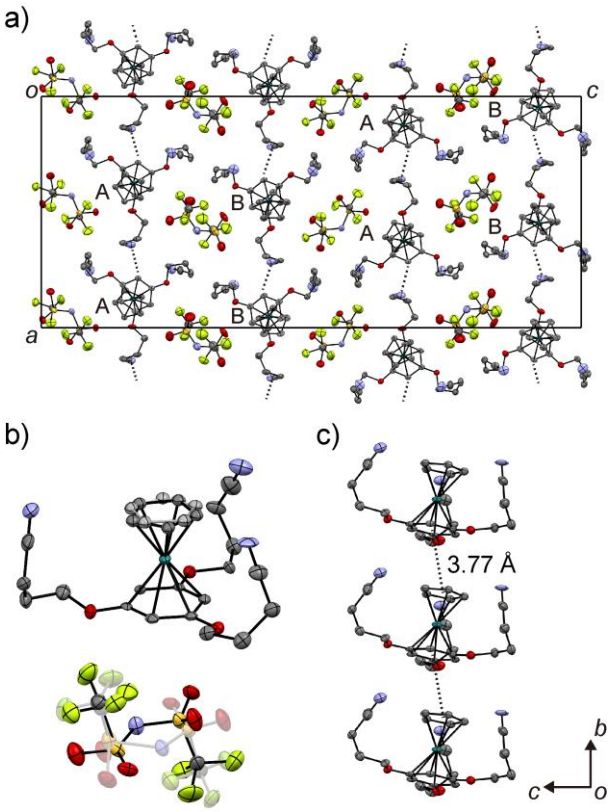

Fig. 7. Crystal structure of **1b** at −173 °C. (a) Packing diagram (*b*-axis projection); (b) molecular structures of cation A and anion A, where the part displayed in gray shows the disordered moieties; and (c) stacking of the cations (cation A). The dotted lines in (a) represent the CN···H

interactions. The dotted lines in (c) represent the centroid-centroid distances.

3. Conclusion

Ru-containing organometallic ILs **1a** and **1b** bearing cyanopropyloxy substituents were synthesized. The substituents were shorter than those in the previously reported photoreactive ILs. Accordingly, the synthesized ILs had high melting points (but lower than 100 °C), enabling crystal structure analysis. The supercooled liquid of **1a** exhibited a photochemical transformation into an amorphous coordination polymer, though the reaction rate was considerably low owing to its high viscosity. The cation did not form a layered structure in either salt, in contrast to the salts with 1,2,3-substituted ligands. The results of the analyses revealed the characteristic features of the ILs, such as anion disorder, intermolecular π–π interactions, CH···N hydrogen-bond-like interactions, and cation structure with substituents surrounding the sandwich complex moiety. These features may affect the physical properties of organometallic ILs and may be partly responsible for their high glass transition temperatures and high melting points. Further, the results of this study are beneficial for the design of photofunctional materials based on Ru-containing organometallic ILs.

4. EXPERIMENTAL

4.1. General

The ^{1}H NMR spectra were recorded on a Bruker Avance 400 MHz spectrometer. The FT–IR spectra were acquired via attenuated total reflectance (ATR), utilizing a Thermo Scientific Nicolet iS5 spectrometer. The DSC measurements were performed on a TA instrument Q100 differential scanning calorimeter at a scan rate of 10 °C min^{-1} using aluminum hermetic pans as sample containers. Photoirradiation of **1a** was carried out with a deep UV lamp (250 W)

using USHIO SP-9 SPOT CURE. The liquid samples were sandwiched between quartz plates during photoirradiation, and the reaction rates were determined from the UV–Vis spectral absorbance at 370 nm and ^{1}H NMR spectra [6].

The single-crystal X-ray diffraction data were collected on a Bruker APEX II Ultra diffractometer with Mo Kα radiation, at −173 and 0 °C. The crystals were cooled at the rate of 2 °C min^{-1}. The structures were solved by the direct method by employing SHELXS [14]. The crystallographic parameters are listed in Table S1. Because of the severe disorder, restraints were applied to the temperature factors of the anion in **1a** at 0 °C, the temperature factors of anion B, the cation Cp rings and the bond lengths of anion B in **1b**.

CCDC 1997224 (**1a**, 100 K), 1997223 (**1a**, 273 K), and 1997222 (**1b**, 100 K) contain the crystallographic data pertaining to this work. These data can be obtained free of charge via www.ccdc.cam.ac.uk/data_request/cif.

4.2. Synthesis

IL **1a** was synthesized by the same method that was employed for the synthesis of the cyanohexyloxy derivative [6], except that 1,3,5-$C_6H_3(OC_3H_6CN)_3$ was utilized as the arene ligand (white solid, yield 35%). The single crystals were prepared by the slow diffusion of diethyl ether into a dichloromethane (DCM) solution of the salt. ^{1}H NMR (400 MHz, $CDCl_3$, TMS): δ = 2.15 (m, 6H, -OCH$_2$C*H*$_2$CH$_2$CN), 2.60 (t, *J* = 6.7 Hz, 6H, -OCH$_2$CH$_2$C*H*$_2$CN), 4.14 (t, *J* = 5.5 Hz, 6H, -OC*H*$_2$CH$_2$CH$_2$CN), 5.39 (s, 5H, Cp), 6.11 (s, 3H, ArH). FT-IR (ATR, cm^{-1}): 569 (s), 740 (m), 825 (m), 1046 (m), 1104 (m), 1174 (vs), 1362 (m), 1379 (m), 1537 (m), 2247 (w). HRMS (ES$^+$): m/z calcd for $[C_{23}H_{26}N_3O_3Ru]^+$ 494.1018, found 494.1034. Anal. Calcd for $C_{23}H_{26}F_2N_4O_7RuS_2$: C, 41.01; H, 3.89; N, 8.32. Found: C, 41.14; H, 3.88; N, 8.14.

IL **1b** was synthesized by the same method, except that $LiTf_2N$ was utilized instead of KFSA for the anion exchange. The product was recrystallized from ethyl acetate–diethyl ether (white

solid, yield 46%). The single crystals utilized for the structural analysis were prepared by the slow diffusion of diethyl ether into a DCM solution of the salt. ^{1}H NMR (400 MHz, $CDCl_3$, TMS): δ = 2.15 (m, 6H, -$OCH_2CH_2CH_2CN$), 2.59 (t, J = 6.7 Hz, 6H, -$OCH_2CH_2CH_2CN$), 4.16 (t, J = 5.7 Hz, 6H, -$OCH_2CH_2CH_2CN$), 5.41 (s, 5H, Cp), 6.13 (s, 3H, ArH). FT-IR (ATR, cm^{-1}): 569 (s), 609 (s), 739 (m), 795 (m), 852 (m), 894 (m), 1046 (s), 1173 (vs), 1350 (m), 1391 (m), 1425 (m), 1537 (s), 2240 (w). Anal. Calcd for $C_{25}H_{26}F_6N_4O_7RuS_2$: C, 38.81; H, 3.39; N, 7.24. Found: C, 38.83; H, 3.34; N, 7.36.

Funding

This work was financially supported by The Canon Foundation and KAKENHI (grant number 20H02756) from the Japan Society for the Promotion of Science (JSPS).

References

[1] M. Kar, K. Matuszek, D. R. MacFarlane, Ionic Liquids. Kirk–Othmer Encyclopedia of Chemical Technology; John Wiley & Sons, Inc. (2019), https://doi.org/10.1002/0471238961.ionisedd.a01.pub2

[2] a) N. R. Brooks, S. Schaltin, K. Van Hecke, L. Van Meervelt, K. Binnemans, J. Fransaer, Copper(I)-Containing Ionic Liquids for High-Rate Electrodeposition, Chem. Eur. J. 17 (2011) 5054–5059, https://doi.org/10.1002/chem.201003209.

b) A. Branco, L. C. Branco, F. Pina, Electrochromic and magnetic ionic liquids, Chem. Commun. 47 (2011) 2300−2302, https://doi.org/10.1039/C0CC03892J.

c) J. Klingele, Low-melting complexes with cationic side chains – Phosphonium-, ammonium- and imidazolium-tagged coordination compounds, Coord. Chem Rev, 292 (2015), 15–29, https://doi.org/10.1016/j.ccr.2015.02.006.

d) L. Ma, C. J. E. Haynes, A. B. Grommet, A. Walczak, C. C. Parkins, C. M. Doherty, L. Longley, A. Tron, A. R. Stefankiewicz, T. D. Bennett, J. R. Nitschke, Coordination cages as permanently porous ionic liquids, Nat. Chem. 12 (2020) 270–275, https://doi.org/10.1038/s41557-020-0419-2.

[3] a) T. Inagaki, T. Mochida, M. Takahashi, C. Kanadani, T. Saito, D. Kuwahara, Ionic Liquids of Cationic Sandwich Complexes, Chem. Eur. J. 18 (2012), 6795–6804, https://doi.org/10.1002/chem.201200151.

b) Y. Funasako, T. Mochida, T. Inagaki, T. Sakurai, H. Ohta, K. Furukawa, T. Nakamura, Magnetic memory based on magnetic alignment of a paramagnetic ionic liquid near room temperature, Chem. Commun. 47 (2011), 4475–4477, https://doi.org/10.1039/C0CC05820C.

[4] a) Y. Funasako, T. Mochida, K. Takahashi, T. Sakurai, H. Ohta, Vapochromic Ionic Liquids from Metal–Chelate Complexes Exhibiting Reversible Changes in Color, Thermal, and Magnetic Properties, Chem. Eur. J. 18 (2012) 11929–11936, https://doi.org/10.1002/chem.201201778.

b) M. Okuhata, Y. Funasako, K. Takahashi, T. Mochida, A spin-crossover ionic liquid from the cationic iron(iii) Schiff base complex, Chem. Commun. 49 (2013) 7662–7664, https://doi.org/10.1039/C3CC44199G.

[5] a) T. Tominaga, T. Ueda, T. Mochida, Effect of substituents and anions on the phase behavior of Ru(ii) sandwich complexes: exploring the boundaries between ionic liquids and ionic plastic crystals, Phys. Chem. Chem. Phys. 19 (2017) 4352–4359, https://doi.org/10.1039/C6CP08308K.

b) T. Ueda, T. Mochida, Thermal Properties and Crystal Structures of Ionic Liquids from Ruthenium Sandwich Complexes with Trialkoxybenzene Ligands: Effects of Substituent Positions and Alkyl Chain Lengths, Organometallics 34 (2015) 1279–1286, https://doi.org/10.1021/acs.organomet.5b00021.

c) R. Fan, R. Sumitani, T. Mochida, Synthesis and Reactivity of Cyclopentadienyl Ruthenium(II) Complexes with Tris(alkylthio)benzenes: Transformation between Dinuclear and Sandwich-Type Complexes, ACS Omega 5 (2020) 2034–2040, https://doi.org/10.1021/acsomega.9b04272.

[6] Y. Funasako, S. Mori, T. Mochida, Reversible transformation between ionic liquids and coordination polymers by application of light and heat, Chem. Commun. 52 (2016) 6277–6279, https://doi.org/10.1039/C6CC02807A.

[7] a) T. Ueda, T. Tominaga, T. Mochida, K. Takahashi, S. Kimura, Photogeneration of Microporous Amorphous Coordination Polymers from Organometallic Ionic Liquids, Chem. Eur. J. 24 (2018) 9490–9493, https://doi.org/10.1002/chem.201801365. b) R. Sumitani, T. Mochida, Metal-containing Poly(ionic liquid) Exhibiting Photogeneration of Coordination Network: Reversible Control of Viscoelasticity and Ionic Conductivity, Macromolecules in press (2020), https://doi.org/10.1021/acs.macromol.0c01141.

[8] R. Sumitani, H. Yoshikawa, T. Mochida, Reversible control of ionic conductivity and viscoelasticity of organometallic ionic liquids by application of light and heat, Chem. Commun. 56 (2020) 6189–6192, https://doi.org/10.1039/D0CC02786C.

[9] a) P. M. Dean, J. M. Pringle, D. R. MacFarlane, Structural analysis of low melting organic salts: perspectives on ionic liquids, Phys. Chem. Chem. Phys. 12 (2010) 9144–9153, https://doi.org/10.1039/C003519J.

b) T. V. Hoogerstraete, N. R. Brooks, B. Norberg, J. Wouters, K. Van Hecke, L. Van Meervelt, K. Binnemans, Crystal structures of low-melting ionic transition-metal complexes with N-alkylimidazole ligands, CrystEngComm 14 (2012) 4902–48911, https://doi.org/10.1039/C2CE25470K.

c) G. Laus, G. Bentivoglio, V. Kahlenberg, K. Wurst, G. Nauer, H. Schottenberger, M. Tanaka, H.-U. Siehl, Conformational Flexibility and Cation–Anion Interactions in 1-Butyl-2,3-dimethylimidazolium Salts, Cryst. Growth Des. 12 (2012) 1838–1846, https://doi.org/10.1021/cg201424m.

d) P. Zürner, H. Schmidt, S. Bette, J. Wagler, G. Frisch, Ionic liquid, glass or crystalline solid? Structures and thermal behaviour of $(C_4mim)_2CuCl_3$, Dalton Trans. 45 (2016) 3327–3333, https://doi.org/10.1039/C5DT03772G.

e) R. Yunis, A. F. Hollenkamp, C. Forsyth, C. M. Doherty, D. Al-Masri, J. M. Pringle, Organic salts utilising the hexamethylguanidinium cation: the influence of the anion on the structural, physical and thermal properties, Phys. Chem. Chem. Phys. 21 (2019) 12288–12300, https://doi.org/10.1039/C9CP01740B.

[10] a) W. A. Henderson, M. Herstedt, V. G. Young, S. Passerini, H. C. De Long, P. C. Trulove, New Disordering Mode for $TFSI^-$ Anions: The Nonequilibrium, Plastic Crystalline Structure of Et_4NTFSI, Inorg. Chem. 45 (2006) 1412–1414, https://doi.org/10.1021/ic0513742.

b) K. Matsumoto, T. Oka, T. Nohira, R. Hagiwara, Polymorphism of Alkali Bis(fluorosulfonyl)amides ($M[N(SO_2F)_2]$, M = Na, K, and Cs), Inorg. Chem. 52 (2013) 568–576, https://doi.org/10.1021/ic3010486.

c) I. A. Shkrob, T. W. Marin, Y. Zhu, D. P. Abraham, Why Bis(fluorosulfonyl)imide Is a "Magic Anion" for Electrochemistry, J. Phys. Chem. C 118 (2014) 19661–19671, https://doi.org/10.1021/jp506567p.

d) T. Mochida, Y. Funasako, T. Inagaki, M. Jiao Li, K. Asahara, D. Kuwahara, Crystal Structures and Phase-Transition Dynamics of Cobaltocenium Salts with Bis(perfluoroalkylsulfonyl)amide Anions: Remarkable Odd–Even Effect of the Fluorocarbon Chains in the Anion, Chem. Eur. J. 19 (2013) 6257–6264, https://doi.org/10.1002/chem.201300186.

e) T. Mochida, Y. Funasako, M. Ishida, S. Saruta, T. Kosone, T. Kitazawa, Crystal Structures and Phase Sequences of Metallocenium Salts with Fluorinated Anions: Effects of Molecular

Size and Symmetry on Phase Transitions to Ionic Plastic Crystals, Chem. Eur. J. 22 (2016) 15725–15732, https://doi.org/10.1002/chem.201603170.

[11] O. Yamamuro, Y. Minamimoto, Y. Inamura, S. Hayashi, H. Hamaguchi, Heat capacity and glass transition of an ionic liquid 1-butyl-3-methylimidazolium chloride, Chem. Phys. Lett. 423 (2006) 371–375, https://doi.org/10.1016/j.cplett.2006.03.074.

[12] a) D. Zhao, Z. Fei, R. Scopelliti, P. J. Dyson, Synthesis and Characterization of Ionic Liquids Incorporating the Nitrile Functionality, Inorg. Chem. 43 (2004) 2197–2205, https://doi.org/10.1021/ic034801p.

b) Z. Fei, D. Zhao, D. Pieraccini, W. H. Ang, T. J. Geldbach, R. Scopelliti, C. Chiappe, P. J. Dyson, Development of Nitrile-Functionalized Ionic Liquids for C−C Coupling Reactions: Implication of Carbene and Nanoparticle Catalysts, Organometallics 26 (2007) 1588–1598, https://doi.org/10.1021/om060950e.

[13] J. Neumann, B. Golub, L.-M. Odebrecht, R. Ludwig, D. Paschek, Revisiting imidazolium based ionic liquids: effect of the conformation bias of the [NTf_2] anion studied by molecular dynamics simulations, J. Chem. Phys., 148 (2018) 193828–193829, https://doi.org/10.1063/1.5013096.

[14] G. M. Sheldrick, A Short History of SHELX. Acta Crystallogr., Sect. A: Found. Crystallogr. 64 (2008) 112–122, https://doi.org/10.1107/S0108767307043930.

Supporting Information

Thermal properties and crystal structures of ruthenium-containing photoreactive ionic liquids with short substituents

Ryo Sumitani,[a] Yusuke Funasako,[a†] Tomoyuki Mochida*[a,b]

[a]*Department of Chemistry, Graduate School of Science, Kobe University, Rokkodai, Nada, Kobe, Hyogo 657-8501, Japan*

[b]*Center for Membrane Technology, Kobe University, Rokkodai, Nada, Kobe, Hyogo 657-8501, Japan*

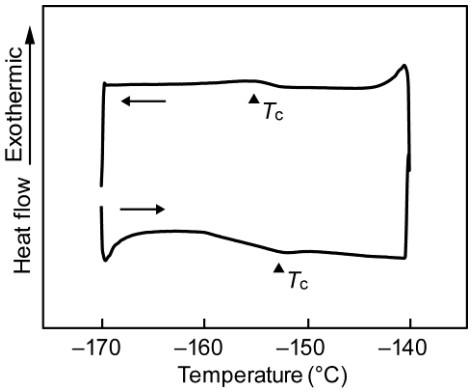

Fig. S1. DSC traces of **1a** in the low temperature region recorded at a scan rate of 5 °C min^{-1}, where T_c indicates the phase transition peak.

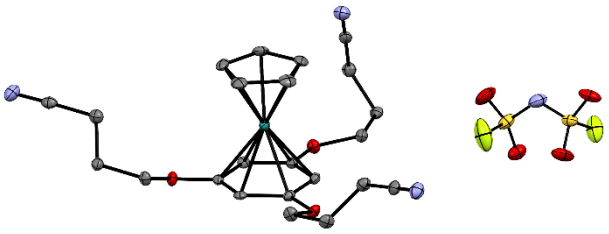

Fig. S2. Molecular structures of cation B and anion B in **1a** at −173 °C. The hydrogen atoms were omitted for clarity.

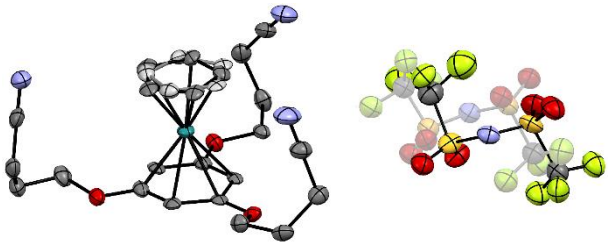

Fig. S3. Molecular structures of cation B and anion B in **1b** at −173 °C. The hydrogen atoms were omitted for clarity. The part displayed in gray represents the disordered moieties.

Table S1. Crystallographic parameters for **1a** and **1b**.

	1a (−173 °C)	**1a** (0 °C)	**1b** (−173 °C)
Empirical formula	$C_{23}H_{26}F_2N_4O_7RuS_2$	$C_{23}H_{26}F_2N_4O_7RuS_2$	$C_{25}H_{26}F_6N_4O_7RuS_2$
Formula weight	673.67	673.67	773.69
Crystal system	Monoclinic	Monoclinic	Orthorhombic
Space group	$P2_1/n$	$P2_1/n$	$Pca2_1$
a (Å)	15.653(2)	7.9875(4)	19.279(4)
b (Å)	18.163(2)	18.2176(9)	7.0227(15)
c (Å)	20.218(3)	18.8031(9)	45.241(10)
α (°)	90	90	90
β (°)	112.705(2)	90.2270(10)	90
γ (°)	90.	90	90
V (Å^3)	5302.6(12)	2736.1(2)	6125(2)
Z	8	4	8
d_{calcd} (mg m^{-3})	1.688	1.635	1.678
T (K)	100	273	100
μ (mm^{-1})	0.814	0.789	0.734
F(000)	2736.0	1368.0	3120.0
Reflections collected	30745	15866	32824
R_{int}	0.0342	0.0249	0.0278
Goodness-of-fit	1.029	1.023	1.107
R_1, wR_2 [$I > 2\sigma$(I)]	0.0402, 0.0981	0.0368, 0.0956	0.0527, 0.1218
R_1, wR_2 (all data)	0.064, 0.1112	0.0488, 0.1037	0.0563, 0.1218
Sample size (μm)	86 × 62 × 36	86 × 62 × 36	119 × 107 × 25